Gas-Phase Reactivity of Lead(II) Ions with D-Glucose. Combined Electrospray Ionization Mass Spectrometry and Theoretical Study

Jean-Yves Salpin* and Jeanine Tortajada

Laboratoire Analyse et Environnement, UMR CNRS 8587, Bâtiment des Sciences, Université d'Evry Val d'Essonne, Boulevard François Mitterrand, 91025 Evry Cedex, France

Received: December 9, 2002; In Final Form: February 26, 2003

The gas-phase reactivity of lead(II) ions toward D-glucose has been studied by means of mass spectrometry and theoretical calculations. Electrospray mass spectra show that this reactivity mainly gives rise to $[Pb(D\text{-glucose})_m - H]^+$ species ($m = 1, 2$). These ions are obtained by dissociative proton transfer within the doubly charged complexes, $[Pb(D\text{-glucose})_n]^{2+}$ complexes ($n = 2-12$), observed in significant abundance at low cone voltage. Low-energy MS/MS experiments on $[Pb(D\text{-glucose}) - H]^+$ (m/z 387) show that this ion essentially dissociates according to cross-ring cleavages leading mainly to the elimination of $C_2H_4O_2$ and $C_4H_8O_4$ neutrals and to a minor extent in the loss of $C_3H_6O_3$. Use of labeled D-glucose demonstrates that the former implies specifically the elimination of C(1) and C(2) stereocenters, whereas the latter corresponds to at least two distinct fragmentations. This finding clearly suggests that several $[Pb(D\text{-glucose}) - H]^+$ structures, characterized by different coordination schemes, coexist in the gas phase. This is confirmed by the density functional theory study carried out on both anomers, because the various coordination sites on the pyranose are close in energy. The most favorable Pb^{2+}/D-glucopyranose association is characterized by the metallic center bonded to the deprotonated hydroxymethyl group and interacting with the hemiacetal oxygen. In such a position, the Pb^{2+} ion catalyzes the ring-opening process by activation of the two C−O ring bonds. This not only accounts for the fragmentation observed upon collision but also suggests that, besides fragmentation, pyranosic complexes may evolve toward energetically favored acyclic structures.

Introduction

From the beginning of the 18th century to the early 1990s, anthropogenic emission of lead has dramatically grown, mainly due to the massive use of alkyllead species as antiknock agents in gasoline and the production of Pb acid storage batteries or leaded paints.[1,2] Both organic lead and inorganic lead are now ubiquitous in the environment, even though, because of the sudden awareness of its toxicity, many countries have significantly reduced during the past decade the use of this metal in numerous industrial fields. These species may indeed cause severe damage to human health. For instance, it has been established that alkylleads are rapidly metabolized and readily cross the blood−brain barrier. These physicochemical properties make the central nervous system the main site of their toxic action. However, lead can also affect almost every organ and system in the human body, such as the liver, kidneys, or heart. Lead is also known to cause weakness of joints and anemia. Because lead readily crosses the placenta, the fetus is at risk. Finally, alkyllead compounds decompose in aqueous solution to give in a final step Pb^{2+} ions,[3] a large-scale environmental pollutant, which is known to obstruct heme biosynthesis, inhibit several zinc enzymes, and interact with nucleic acids and transfer RNA, affecting protein synthesis.[4]

The bioavailability and toxicity of metals in the environment are governed by the ability of natural organic molecules to bind metal ions. Among these molecules carbohydrates are the most abundant. They are mainly found as polysaccharides that are essential for both plant and animal life. These macromolecules may be easily converted to a large variety of monosaccharides, which, in turn, may complex metal ions due to their numerous hydroxyl groups. Complexing of carbohydrates with metal ions, and more particularly with Ca^{2+} cations, has been widely studied in solution[5,6] because of the involvement of metal ion−saccharide interactions in key biological processes. On the other hand, studies concerning the interactions of Pb^{2+} ions with saccharides in aqueous media are scarce and generally concern determination of thermochemical parameters such as stability constants or heats of reaction.[7−10] The intimate mechanism of interaction is not well characterized. Moreover, these complexation processes depend on many parameters of aqueous media, such as pH, ionic strength, or metal/ligand ratio. Therefore, to properly assess the influence of each of these parameters, it is of particular interest to describe in a first step the gas-phase reactivity of metallic cations. Our previous studies have demonstrated that the gas-phase reactivity of Pb^{2+} ions allows isomeric hexoses and pentoses to be characterized,[11−13] thus underscoring the influence of the arrangement of the various hydroxyl groups on the complexation process. The present work aims to explore the mechanical aspects of the gas-phase interaction between Pb^{2+} ions and the most abundant monosaccharide, D-glucose (Scheme 1). For this purpose, we combined mass spectrometry experiments, notably on deoxy and labeled species, with theoretical calculations.

Experimental Section

Electrospray mass spectra were recorded on an Applied Biosystems/MDS Sciex API2000 triple-quadrupole instrument fitted with a "turboionspray" ion source. Samples were intro-

* Corresponding author (telephone 33 1 69 47 76 47; fax 33 1 69 47 76 55; e-mail Jean-Yves.Salpin@chimie.univ-evry.fr).

10.1021/jp022553x CCC: $25.00
Published on Web 04/01/2003

SCHEME 1

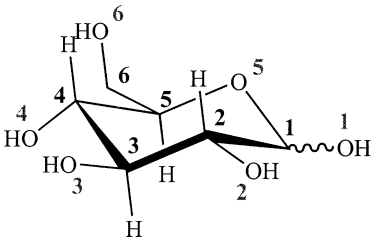

duced into the source using direct infusion with a syringe pump, at a flow rate of 5 μL/min. Ionization of the samples was achieved by applying a voltage of 5.5 kV on the sprayer probe and by the use of a nebulizing gas (GAS1, air) surrounding the sprayer probe, intersected by a heated gas (GAS2, air) at an angle of ~90°. The operating pressures of these two gases were typically 1.4 and 2.1 bar, respectively, and the temperature of GAS2 was set at 100 °C. The curtain gas (N_2), which prevents air or solvent from entering the analyzer region, was adjusted to a pressure of 2.1 bar. As detailed in the following sections, the declustering potential (DP), defined as the difference of potentials between the orifice plate and the skimmer, was fixed to 20 V to perform both MS and MS/MS experiments.

MS/MS spectra were carried out by introducing nitrogen as collision gas in the second quadrupole at a total pressure of 4 $\times$ 10^{-5} mbar, the background pressure being ~10^{-5} mbar. Furthermore, MS/MS spectra were systematically recorded at different collision energies (the collision energy is given by the difference of potentials between the focusing quadrupole Q0 preceding Q1 and the collision cell Q2).

All of the measurements presented hereafter were carried out in 100% water purified with a Milli-Q water purification system. Lead nitrate was chosen to generate Pb^{2+} ions because of its high solubility in water. All of the monosaccharides were dissolved in water without any preliminary derivatization. The resulting pH of our aqueous mixtures of lead nitrate/D-glucose (5×10^{-5} mol·L^{-1}/10^{-4} mol·L^{-1}) was ~5, similar to that of Milli-Q water.

Metallic salt, D-glucose, and deoxy-D-glucoses are commercially available from Aldrich and Fluka (Saint-Quentin Fallavier, France) and were used without any further purification. ^{13}C- and deuterium-labeled D-glucoses were obtained from Omicron Biochemicals (South Bend, IN).

Computational Details

Due to the large number of atoms involved in the complexes studied, molecular orbital calculations have been undertaken using the B3LYP density functional approach, as implemented in the Gaussian 98 set of programs.[14] This method combines Becke's three-parameter nonlocal hybrid exchange potential[15] with the nonlocal correlation function of Lee, Yang, and Parr.[16] This formalism has been found to be well suited both for description of ion−molecule complexes[17−19] and for the study of inter- and intramolecular hydrogen bonds.[19−22] The different structures have first been optimized with the dp-polarized 6-31G(d,p) basis set for C, H, and O atoms. Harmonic vibrational frequencies have been determined at that level. Finally, relative energies were determined using the extended basis set 6-311+G(2df,2p).

Different effective core potentials (ECP) have been proposed in the literature for Pb. In the present study, we used the "Stuttgart" quasi-relativistic pseudo-potential developed by Küchle et al.[23] This particular ECP employs a (*4s,4p,1d*)/[*2s,2p,1d*] basis set with a (3,1) contraction scheme for *s* and *p* functions. Hence, this basis set can be used directly in conjunction with the standard 6-31G(d,p) Pople basis set of C, O, and H for geometry optimization. To perform calculations at a higher level of theory, we have uncontracted the original scheme of the Stuttgart basis set to obtain a triple-ζ-like basis set, with a (2,1,1) contraction scheme for *s* and *p* functions. Furthermore, this basis set was supplemented with one *d* polarization function and one *f* polarization function (α_d = 0.195, α_f = 0.375) and an *sp* diffuse function (α_{sp} = 0.033).[24] To create a multiple set of *d* functions from a single optimized function, we have followed the procedure previously described by González et al.[25] in which the new exponents are obtained as multiples, $n\alpha_d$, or fractions, α_d/n, of the single exponent α_d, with n = 1.5. This modified basis set has been used together with the C, H, and O 6-311+G(2df,2p) basis set for single-point calculations. For simplicity in nomenclature, the basis sets used for Pb in conjunction with the 6-31G(d,p) and 6-311+G(2df,2p) for the remaining atoms will now be referred to as 6-31G(d,p) and 6-311+G(2df,2p) basis sets, respectively.

Throughout this paper total energies are expressed in hartrees and relative energies in kilojoules per mole. Unless otherwise noted, the relative energies given hereafter are those obtained at a level equivalent to B3LYP/6-311+G(2df,2p)//B3LYP/6-31G(d,p)+ZPE. Detailed geometries of all the structures mentioned in this paper are available as Supporting Information.

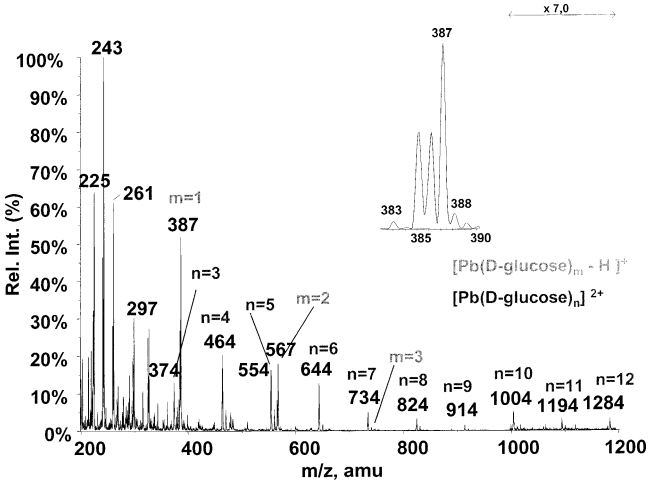

Figure 1. *m*/*z* 200−1200 range of the positive-ion electrospray mass spectrum of an aqueous $Pb(NO_3)_2$/D-glucose (5×10^{-5} mol·L^{-1}/5×10^{-4} mol·L^{-1}) solution. For the sake of clarity, peaks at *m*/*z* 279 and 284 are not labeled (see text for details).

Results

Positive Ion Electrospray Spectra of Cationized Glucose. Figure 1 presents the *m*/*z* 200−1200 range of the electrospray mass spectrum obtained at a declustering potential of 20 V when an aqueous lead nitrate/D-glucose mixture (5×10^{-5} mol·L^{-1}/5×10^{-4} mol·L^{-1}) was infused. Lead has four isotopes with the following natural abundances: 1.4% ^{204}Pb, 24.1% ^{206}Pb, 22.1% ^{207}Pb, and 52.4% ^{208}Pb. Because of this specific isotopic distribution (Figure 1), peaks involving one lead atom correspond to characteristic triplets on the spectra and are easily identified (to simplify, we shall not consider the very weak ^{204}Pb contribution). Unless otherwise noted, throughout this paper the *m*/*z* of any metal-containing ion will always refer to the one containing the metal isotope of highest natural abundance (^{208}Pb). From Figure 1, we can see that the electrospray spectrum, at DP = 20 V, presents hydrated lead hydroxide ions $PbOH^+ \cdot xH_2O$ (x = 0−4 at *m*/*z* 225, 243, 261 279, and 297).

TABLE 1: Low-Energy CID Spectra of a Series of $[Pb(D\text{-glucose})_n]^{2+}$ Ions ($n = 2-6$)[a]

	precursor ion				
product ion	*m*/*z* 284 ($n = 2$)	*m*/*z* 374 ($n = 3$)	*m*/*z* 464 ($n = 4$)	*m*/*z* 554 ($n = 5$)	*m*/*z* 644 ($n = 6$)
$(glc)H^+$ (*m*/*z* 181)[b]	+[c]	+	+	+	+
$(glc)_2H^+$ (*m*/*z* 361)	−[d]	+	+	+	+
$[Pb(glc) - H]^+$ (*m*/*z* 387)	+	+	+	+	+
$[Pb(glc)_2 - H]^+$ (*m*/*z* 567)	−	+	+	+	+
$[Pb(glc)]^{2+}$ (*m*/*z* 194)	−	−	−	−	−
$[Pb(glc)_2]^{2+}$ (*m*/*z* 284)	nr[e]	−	−	−	−
$[Pb(glc)_3]^{2+}$ (*m*/*z* 374)	nr	nr	+	+	+
$[Pb(glc)_4]^{2+}$ (*m*/*z* 464)	nr	nr	nr	+	+
$[Pb(glc)_5]^{2+}$ (*m*/*z* 554)	nr	nr	nr	nr	+

[a] Recorded with an aqueous solution of $Pb(NO_3)_2$/D-glucose (2×10^{-5} mol·L^{-1}/10^{-4} mol·L^{-1}). [b] glc = D-glucose. [c] Observed. [d] Not observed. [e] Not relevant.

Low-energy collision-induced dissociation (CID) spectra of these hydrated hydroxide ions are characterized by the loss of one or several molecules of water. Elimination of OH is never observed, suggesting that the binding energy of OH is greater than that of water, as already observed for transition metals such as Mn, Co, Ni, or Zn.[26] Increasing the declustering potential up to 200 V results in the gradual removal of hydrated hydroxide ions. Conversely, bare lead ion Pb^+ (*m*/*z* 208), originating from $PbOH^+$ by loss of a hydroxyl radical, starts to appear at DP = 50 V, to become the base peak at the highest DP.

Numerous studies have shown that electrospray ionization can be used to generate hydrated divalent metal ions $M(H_2O)_n^{2+}$.[27−33] Furthermore, these ions may easily dissociate either by water loss or by formation of metal hydroxide ions according to the following dissociative proton-transfer reaction (eq 1):

$$M(H_2O)_n^{2+} \rightarrow MOH(H_2O)_{n-k-2}^{+} + H_3O^+(H_2O)_k \quad (1)$$

The second ionization potential of the metal (IP_2) has been proposed as one of the determining factors for both the formation of hydrated metals and their fragmentation according to this proton-transfer reaction.[27−29] However, in a recent paper, Williams and co-workers deduced from their experiments that its influence was only indirect[32] and put forward the key role of the ionic radius.[32,34] Hence, metal hydroxide formation is particularly favorable as the size of the metal ion decreases. In the present study, we did not detect any $Pb(H_2O)_n^{2+}$ ions, but only $PbOH(H_2O)_n^+$ ions ($n = 1-4$) species. This is quite striking because lead has the same IP_2 as magnesium [IP_2(Pb) = 15.03 eV[35]] and an ionic radius similar to that of strontium[35] (whatever the coordination number considered), two metals for which hydrated metal ions are easily obtained under electrospray conditions.

On the other hand, as Kebarle and co-workers noticed, the proton-transfer reaction (eq 1) is also facilitated by collisions between the hydrated metal and gas molecules in the interface region.[27−29] We tried to record spectra with the mildest source/interface conditions (DP = 0 V, low curtain and heated gases) but again failed in detecting any hydrated lead ions. A possible explanation could involve the composition of the aqueous solution of lead nitrate. For instance, Shvarstburg et al. did not manage to produce $Sn(H_2O)_n^{2+}$ ions by electrospray and deduced from equilibrium calculations that this was not so surprising because $SnOH^+$ ions should represent 99.4% of the ionic species in a 2 mM solution.[36] The pH of our lead nitrate solutions, when using Milli-Q water, ranged from 3 to 5, for $Pb(NO_3)_2$ concentrations spanning from 10^{-3} to 10^{-5} mol·L^{-1}. According to a recent potentiometric study,[37] Pb^{2+} ions are the predominant ionic species at pH ≤5 for those concentrations. Consequently, the lack of $Pb(H_2O)_n^{2+}$ ions cannot be attributed to the properties of the aqueous solution.

In a recent paper, Stace and co-workers used the pick-up method to generate gas-phase $Pb(ROH)_n^{2+}$ ions.[38] They also failed to detect any $Pb(H_2O)_n^{2+}$ ions but managed to observe doubly charged species with propan-1-ol and butan-1-ol. These experiments, complemented by DFT calculations, allowed them to deduce that the stability of $Pb(ROH)_4^{2+}$ could be explained by the hard−soft acid−base (HSAB) concept.[39] Increasing the length of the alkyl chain indeed results in the softening of the base, a decrease in the ionic character of the Pb−O bond, and a greater stabilization of $Pb(ROH)_4^{2+}$ ions. Our results, although obtained with a different ionization technique, confirm these findings. Whereas no doubly charged ions are observed with water, the contrary is the case with D-glucose, a highly polarizable (soft) base, with which we observe a series of [|Pb-(D-glucose)$_n$]$^{2+}$ ions ($n = 2-12$; *m*/*z* 284, 374, 464, 554, 644, 734, 824, 914, 1004, 1094, and 1184), despite the great excess of water (Figure 1). The detection of these doubly charged species further confirms the presence of Pb^{2+} ions in the aqueous solution. Interaction between lead(II) ions and D-glucose also results in ions of the general formula $[Pb(D\text{-glucose})_m - H]^+$ ($m = 1, 3$) (Figure 1), at *m*/*z* 387, 567, and 747. This double reactivity has been already observed for alkaline earth cations[40] and iron.[41] We optimized the yield of formation of cationized species as previously reported.[13] The highest ionization yield is obtained for a metal/D-glucose ratio of 1/2 (5×10^{-5} mol·L^{-1}/10^{-4} mol·L^{-1}) and a declustering potential of 20 V. Whatever the ratio considered, $[Pb(monosaccharide)_m - H]^+$ ions are predominant and *m*/*z* 387 ($m = 1$) is always the most abundant complex observed. Nevertheless, the metal/monosaccharide ratio has a significant influence on the detection of the doubly charged species, because we observed only six [Pb(D-glucose)$_n$]$^{2+}$ ions ($n = 2-7$) for the stoichiometry 1/2. Therefore, the metal/monosaccharide ratio influences the relative abundance of these two series, but the effect is not as spectacular as for Ca^{2+} ions.[40]

We tried to characterize the structure of these doubly charged species by recording the low-energy CID spectra of *m*/*z* 284, 374, 464, 554, and 644 ions (for a metal/sugar ratio of 1/5). The results are summarized in Table 1. These species exhibit the same behavior upon collision as $M(H_2O)_n^{2+}$ ions. Two main dissociation channels are indeed observed: (i) elimination of one or several glucose units leading to doubly charged ions and (ii) proton transfer within the complex, giving rise to $[Pb(D\text{-glucose})_m - H]^+$ ions ($m = 1$ or 2) together with $(D\text{-glucose})_pH^+$ ($p = 1$ or 2). These product ions further dissociate by elimination of $C_2H_4O_2$ and one or several molecules of water, respectively.

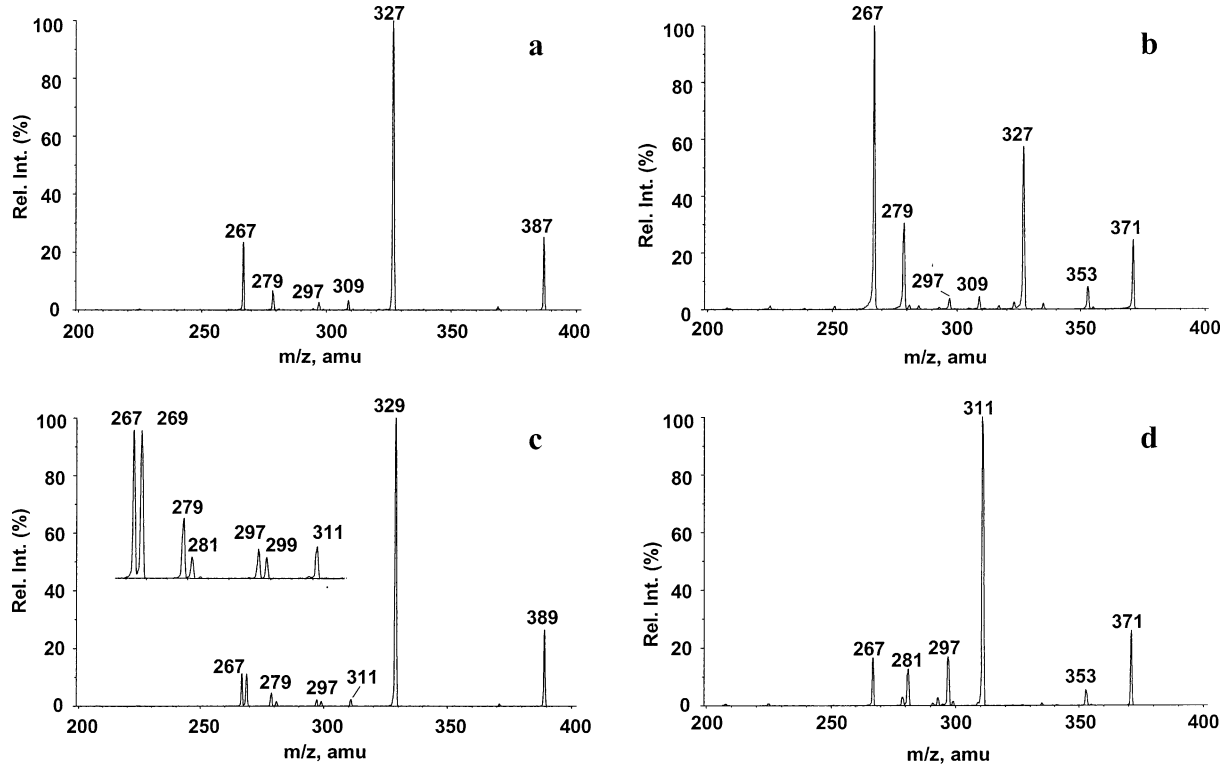

Figure 2. Low-energy CID spectra of [Pb(hexose) − H]$^+$ ions, the hexose being (a) D-glucose, (b) 2-deoxy-D-glucose, (c) [6,6-^{2}H]-D-glucose, and (d) 6-deoxy-D-glucose.

The first process is not observed for ions *m*/*z* 284 and 374. This result therefore suggests that Pb^{2+} ions might strongly interact with three molecules of D-glucose in the first coordination shell and are surrounded by the other glucoses via intermolecular hydrogen bonds (outer coordination sphere).

The charge separation process therefore constitutes the mechanism of formation of [Pb(D-glucose)$_m$ − H]$^+$ ions (m = 1 or 2). It is the main dissociation channel, except for *m*/*z* 644. Moreover, because we do not detect protonated trimers or tetramers of D-glucose, ions *m*/*z* 387 and 567 certainly correspond to consecutive fragmentations from *m*/*z* 644 and 554 (and 464 in the case of *m*/*z* 387). Furthermore, additional MS/MS experiments have demonstrated that *m*/*z* 387 also originates from *m*/*z* 567 by loss of a D-glucose unit. One may also reasonably rule out the proton abstraction reaction (eq 2)

$$Pb^{2+} + \text{D-glucose} \rightarrow [Pb(\text{D-glucose}) - H]^+ + H^+ \quad (2)$$

because Pb^{2+}, if formed in the interface region, would certainly react dissociatively with the D-glucose molecule. Finally, a condensation reaction between lead(II) ions and anionic forms of D-glucose can be also discarded, given the acidic pH of our solutions.

In summary, these data have demonstrated that the [Pb(D-glucose) − H]$^+$ ion (*m*/*z* 387) is the main complex observed under electrospray conditions, and the paper will now focus on its structural characterization, by means of MS/MS experiments, labeled D-glucose, and theoretical calculations.

Low-Energy CID Spectra of [Pb(D-Glucose) − H]$^+$ Ion (*m*/*z* 387). The [Pb(D-glucose) − H]$^+$ species involving ^{208}Pb (*m*/*z* 387) was selected and allowed to dissociate upon collision with nitrogen. MS/MS spectra were systematically recorded at different collision energies between 1 and 30 eV in the laboratory frame. This corresponds to center of mass collision energies (E_{cm}) ranging from 0.07 to 2.02 eV with nitrogen as target gas. The MS/MS spectrum obtained at E_{cm} = 0.9 eV is presented in Figure 2a. The [Pb(D-glucose) − H]$^+$ ion essentially fragments according to cross-ring cleavages, characterized by elimination of $C_nH_{2n}O_n$ molecules (n = 2−4) and leading to 327, 297, and 267 ions. These dissociation processes have been already observed both under FAB and electrospray conditions for glucose derivatized with polyamines and cationized by various divalent transition metal ions such as Ni(II),[42,43] Zn(II),[43,44] Cu(II),[43] or Co(II).[45] These fragmentations are also encountered when Fe(II) ions interact with underivatized D-glucose.[46] Additional MS/MS spectra, including precursor ion scan mode and neutral loss experiments, result in the following fragmentation pattern (Scheme 2).

SCHEME 2

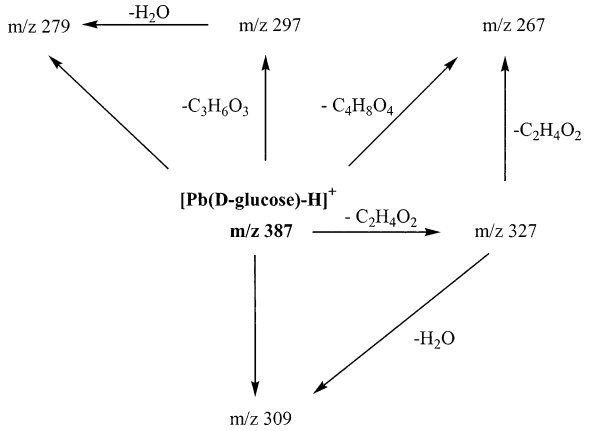

This shows that formation of 297 ions corresponds to a primary fragmentation, elimination of formaldehyde from *m*/*z* 327 being not observed. Elimination of $C_3H_6O_3$ appears to be very minor as already observed with various metallic centers such as Cu, Ni, and Co[45] or Fe.[46] Furthermore, *m*/*z* 267 ions arise either directly from the parent ion or via the intermediate formation of *m*/*z* 327 ions. The reactivity of Pb(II) ions also

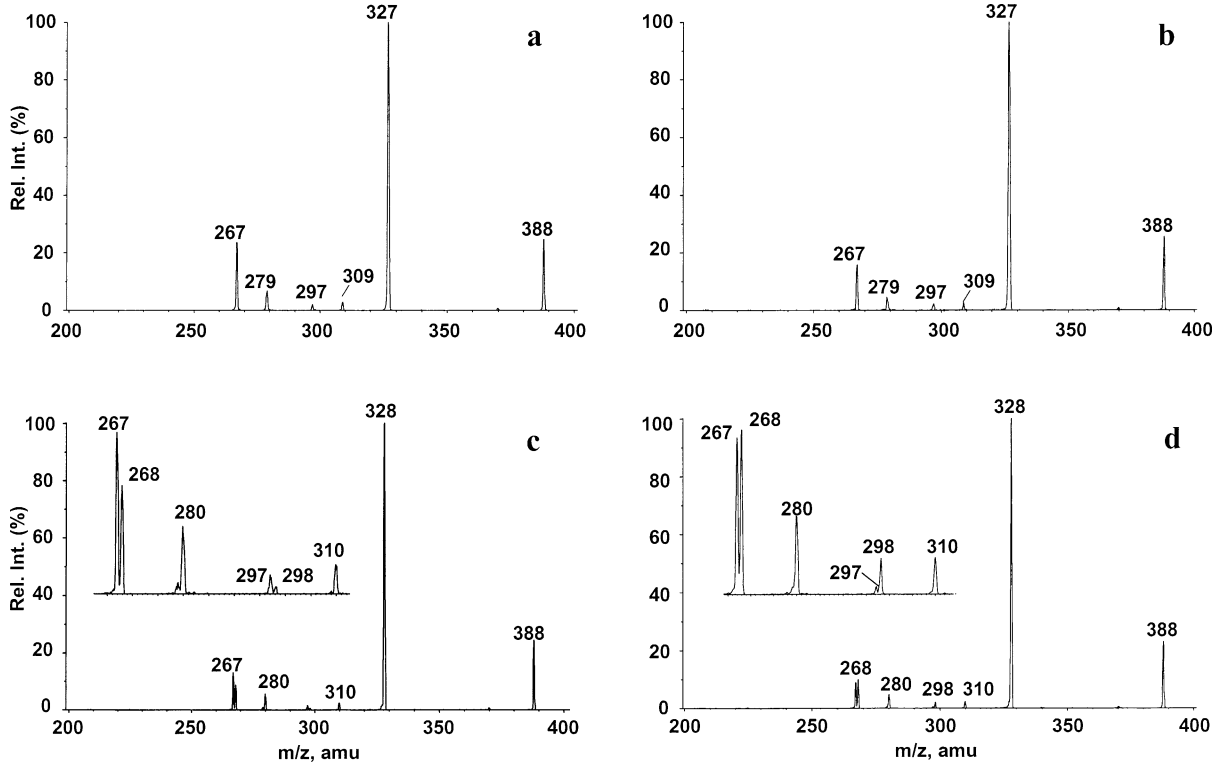

Figure 3. Low-energy CID spectra of [Pb([x-^{13}C]-D-glucose) − H]$^+$ ions, with x = (a) 1, (b) 2, (c) 3, and (d) 5.

TABLE 2: MS/MS Spectra Obtained with Labeled D-Glucose (Loss of Label Is Indicated in Bold)

		product ion (*m*/*z*)				
precursor ion [Pb(D-glucose) − H]$^+$		$-C_2H_4O_2$	$-C_2H_4O_2/-H_2O$	$-C_3H_6O_3$	$-C_3H_6O_3/-H_2O$	$-C_4H_8O_4$
not labeled	*m*/*z* 387	327	309	297	279	267
1-^{13}C	*m*/*z* 388	**327**	**309**	**297**	**279**	**267**
2-^{13}C	*m*/*z* 388	**327**	**309**	**297**	**279**	**267**
2-^{2}H	*m*/*z* 388	**327**	**309**	**297**	**279**	**267**
3-^{13}C	*m*/*z* 388	328	310	**297**/298	**279**/280	**267**/268
5-^{13}C	*m*/*z* 388	328	310	**297**/298	**279**/280	**267**/268
6,6-^{2}H	*m*/*z* 389	329	311	**297**/299	**279**/281	**267**/269

induces particular dissociation processes, corresponding to simultaneous elimination of H_2O and $C_nH_{2n}O_n$ (n = 2, 3) neutrals. This has been observed before only in the case of copper cationization combined with use of ethylenediamine.[43] In fact, precursor ion scan mode and neutral loss experiments suggest that the resulting ions, that is, *m*/*z* 309 and 279, are also generated via intermediate formation of *m*/*z* 327 and 297 ions, respectively. Unlike under FAB/metastable conditions,[12] dehydration from [Pb(hexose) − H]$^+$ ions is a very minor process. Finally, we do not detect any neutral fragments retaining the metal.

To propose reliable mechanisms for the cross-ring cleavages, and subsequently structures for [Pb(D-glucose) − H]$^+$ ions, we undertook additional MS/MS experiments using both deoxy-D-glucoses and glucose labeled either by ^{13}C or by deuterium. The resulting spectra are presented in Figures 2 and 3.

Loss of $C_2H_4O_2$. Elimination of $C_2H_4O_2$ is the predominant process under FAB/metastable conditions.[12] Although the ionization step is different, this suggests that this fragmentation requires a very small amount of energy to occur.

During a previous study,[13] use of 1-*O*-methyl-D-glucoses indicated that the anomeric center could be involved in the fragmentation, because loss of $C_2H_4O_2$ was changed to $C_3H_6O_2$ when a methoxyl group replaced the anomeric hydroxyl. If so, one may reasonably assume that the second carbon involved in $C_2H_4O_2$ could correspond to C(2), insofar as elimination of $C_2H_4O_2$ involving C(1) and not C(2) would require a considerable rearrangement during the dissociation. This is supported by the MS/MS spectrum of [Pb(2-deoxy-D-glucose) − H]$^+$ complex (Figure 2b), which is characterized by exclusive elimination of a C_2H_4O neutral (*m*/*z* 327), whereas a loss of 60 mass units is still observed with 6-deoxy-D-glucose (*m*/*z* 311, Figure 2d). In summary, the experiments carried out with deoxy-D-glucoses are in favor of the elimination of C(1) and C(2) stereocenters. However, as nothing proves that glucose and deoxyglucoses interact with Pb^{2+} ions in the same way, we have undertaken an extensive labeling study. This study is illustrated by Figures 2c and 3 and the results are summarized in Table 2. As just mentioned, loss of a $C_2H_4O_2$ unit without extensive rearrangement requires two adjacent carbon atoms to be expelled. This may correspond to four distinct cross-ring cleavages, implying either elimination of an ethene-1,2-diol unit (HO−CH═CH−OH) or loss of a glyoxal molecule $HOCH_2$−(CO)H. First, we can remark that, whatever the labeled monosaccharide studied, elimination of $C_2H_4O_2$ corresponds to a single peak in the spectra (Figures 2c and 3). This supports the assumption of adjacent carbons eliminated. Second, careful examination of Table 2 clearly demonstrates that the loss of $C_2H_4O_2$ involves exclusively the elimination of the C(1) and

SCHEME 3

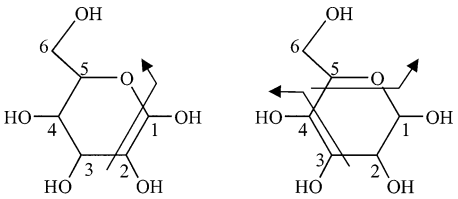

C(2) stereocenters (Scheme 3), thus confirming the results obtained with deoxy-D-glucoses.

This mechanism formally corresponds to ^{0,2}A fragmentation according to the Domon and Costello convention.[47] This result may also suggest that Pb^{2+} ions interact with the ring oxygen and one or several of the hydroxyl groups borne by carbon atom 3, 4, or 6 (Scheme 1) prior to fragmentation.

Loss of $C_4H_8O_4$. Elimination of $C_4H_8O_4$ may also arise from four possible cross-ring cleavages. Nevertheless, a striking feature compared to the elimination of 60 mass units is that this process generates two peaks in MS/MS spectra when using [6,6-^{2}H], [3-^{13}C]-, and [5-^{13}C]-D-glucose (Figures 2c and 3c,d; Table 2). Conversely, a single peak is observed when the isotope is located at position 1 or 2, hence demonstrating that C(1) and C(2) are systematically eliminated (Scheme 3). In addition, examination of Table 2 shows that in a single-step process, these two atoms are expelled together with either C(3)+(C4) (the Pb^{2+} ion interacting with CH_2OH) or C(5)+C(6) [with the metallic center bound to OH(3) and OH(4)]. Losses of C(2) and C(6) atoms are further confirmed by the MS/MS spectra obtained with 2-deoxy- and 6-deoxy-D-glucose, respectively (elimination of $C_4H_8O_3$, 104 Da). Our findings are not only in agreement with the intermediate formation of an ion *m*/*z* 327 by elimination of $C(1)C(2)H_4O_2$ but also clearly suggest that several structures, characterized by different coordination schemes, coexist in the gas phase. This seems to be reasonable because the interligand proton transfer associated with the charge separation process undergone by the $[Pb(D\text{-glucose})_n]^{2+}$ ions should involve one of the hydroxylic protons, which are of comparable acidity.[48]

Loss of $C_3H_6O_3$. As already noted, elimination of $C_3H_6O_3$ is a very minor process, which was not observed under FAB/MIKE conditions.[12] For this particular fragmentation, the spectra obtained with labeled D-glucose are not conclusive. Loss of label observed in Figure 3a−c supports the elimination of the C(1)−C(2)−C(3) chain. The spectrum obtained with [5-^{13}C]-D-glucose leads to the same conclusion (Table 2). However, as two peaks are observed in Figures 2c and 3c,d, formation of *m*/*z* 297 ions certainly arises from at least two mechanisms.

In summary, the data obtained during this study gave useful information concerning the two main cross-ring cleavages. Moreover, these results also indicate that gaseous $[Pb(D\text{-glucose}) - H]^+$ ions may correspond to a mixture of several structures.

Computational Study

Our experiments have demonstrated that the main dissociation processes correspond to the elimination of $C_2H_4O_2$ and $C_4H_8O_4$. These fragmentations are already observed at the lowest collision energy (0.07 eV), even with a very low pressure of nitrogen and a declustering potential set to 0 V (in fact, the declustering potential has no effect on the MS/MS spectra observed). It is commonly admitted that electrospray is a "soft" ionization technique compared to other techniques such as LSIMS or MALDI and that the amount of internal energy imparted to generated ions is the lowest of all mass spectrometric ionization techniques.[49] Moreover, precursor ions having a sufficient lifetime to reach the second quadrupole should be stable prior to collisional activation. Therefore, we have considered that the $[Pb(D\text{-glucose}) - H]^+$ ions are stable species and that our experiments could be carried out in conjunction with ground-state theoretical calculations. These calculations were performed to locate the best coordination sites and, subsequently, to propose possible mechanisms associated with the formation of *m*/*z* 327 and 267 ions.

In water, D-glucose involves almost exclusively[50] (>99%) an equilibrium between the two anomeric α and β cyclic pyranose hemiacetals in their $^4C_1$ chair conformations (as represented in Scheme 1). Consequently, we assumed in a first step that these pyranose rings remain intact during the electrospray process and that Pb^{2+} ions interact initially with $^4C_1$ structures of both anomers. Given the facts that a deprotonation occurs and that metallic species may in principle attach to any of the electron-rich centers of D-glucose, including the hemiacetal oxygen, a considerable number of possible geometries should be considered. To restrict the number of structures investigated, we took into account the observations made during the studies of Na^+/D-glucose[51] and Cu^+/D-glucose[19] systems by considering only bidentate or higher dentate modes and by maximizing intramolecular hydrogen bondings in the complex.

Given the size of this system, an extensive study consisting of PM3 semiempirical calculations[52] was carried out in a preliminary step. The most stable structures were then reoptimized at the B3LYP/6-31G(d,p) level. The results obtained with these two methods are in good agreement.

To describe the various structures, we adopted the nomenclature illustrated by Scheme 4.

We attributed a letter to each of the oxygen atoms. For example, a structure in which lead interacts with the anomeric center, the hydroxymethyl group (CH_2OH), and the hemiacetal oxygen is described by the formalism **AEF**. By convention, the first letter always refers to the deprotonated site.

To define the orientation of the hydroxyl groups, we have used a modified form of the nomenclature introduced by Cramer and Truhlar.[53] This involves a six-letter descriptor, in which the letters correspond to the orientation of the hydroxymethyl group (CH_2OH), followed by that of the C(6), C(4), C(3), C(2), and finally C(1) hydroxyl groups. The hydroxymethyl conformations are defined using the capital letters $\bar{G}$, G, and T and the hydroxyl conformations by the letters $\bar{g}$, g, and t, as reported previously.[53] Each letter indicates whether the H−O−C(*n*)−C(*n*−1) dihedral angle [or the O(6)−C(6)−C(5)−O dihedral for CH_2OH] is gauche(−) [$\bar{g}$, $\bar{G}$], gauche(+) [g, G], or trans [t, T]. According to the Cramer and Truhlar convention, gauche(−) means that a counterclockwise [viewed in the O-to-C(*n*) direction] rotation of the OH (or CH_2OH) of ∼60° is required to eclipse the bond C(*n*)−C(*n*−1) [or C(5)−O], whereas for gauche(+) the rotation is clockwise. With this convention, the $^4C_1$ chair conformation of α-D-glucose depicted in Scheme 4 is associated with the descriptor Tg g $\bar{g}$ $\bar{g}$ g. Finally, the letter x characterizes the deprotonated site, as introduced by Mulroney et al.[48]

B3LYP total and relative energies of the different cyclic structures are summarized in Table 3. For some of them, relevant bond lengths are given in Figures 4 and 5 (for α and β anomers, respectively). Detailed geometries as well as Cartesian coordinates of the various structures studied at the B3LYP level are given in the Supporting Information.

Cyclic Forms of $[Pb(D\text{-glucose}) - H]^+$ Ions. First, from

SCHEME 4

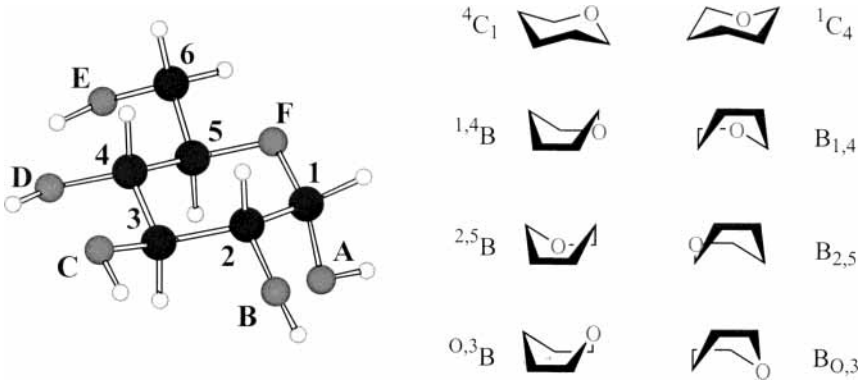

TABLE 3: Total and Relative Energies for the Pyranosic Structures of the [Pb(D-glucose) − H]$^+$ Complex

structure	OH conf[a]	E_1[b] (hartree)	ZPE[b]	ΔE_1 (kJ/mol)[b,c]	E_2[d] (hartree)	ΔE_2 (kJ/mol)[c,d]
α anomer						
α_$^4C_1$_AB	T t t t x	−689.813397	492.2880	27.4	−690.068160	25.2
α_$^4C_1$_BA	T g g $\bar{g}$ x g	−689.802291	490.3289	54.6	−690.061478	44.5
α_$^4C_1$_BC	T t t x g	−689.817329	492.8957	17.6	−690.075769	9.6
α_$^4C_1$_CB	T g g x $\bar{g}$ g	−689.806775	492.5473	45.0	−690.064883	34.1
α_$^4C_1$_CD	T t t x t g	−689.816885	491.1358	17.0	−690.074961	6.2
α_$^4C_1$_DC	T g x $\bar{g}$ $\bar{g}$ g	−689.810312	492.7064	35.9	−690.068315	25.2
α_$^4C_1$_DE	T t x t t t	−689.807042	490.4122	42.2	−690.067012	26.4
α_$^4C_1$_ED	T x g $\bar{g}$ $\bar{g}$ g	−689.819551	492.7896	11.7	−690.077687	4.4
α_$^4C_1$_EFA	G$\bar{x}$ t t t t	−689.815232	490.9892	21.2	−690.073657	9.5
α_$^4C_1$_EF	G$\bar{x}$ g $\bar{g}$ $\bar{g}$ g	−689.807758	491.2090	41.1	−690.067005	27.2
α_$^1C_4$_EF	G$\bar{x}$ $\bar{g}$ t t $\bar{g}$	−689.814465	493.2864	25.6	−690.069989	21.4
α_$B_{O,3}$_EF	G$\bar{x}$ g t t $\bar{g}$	−689.812434	490.5085	28.1	−690.070602	17.0
α_$B_{2,5}$_EFA	G$\bar{x}$ g $\bar{g}$ t $\bar{g}$	−689.814950	490.3239	21.3	−690.071795	13.7
α_^{O,3}B_EFC	G$\bar{x}$ $\bar{g}$ t g g	−689.821921	493.0556	5.7	−690.077380	1.8
α_^{2,5}B_DFA	T$\bar{g}$ x t t t	−689.808894	492.4364	39.3	−690.063178	38.5
α_$B_{1,4}$_DFA	G$\bar{g}$ x t g t	−689.815118	493.7272	24.3	−690.066972	29.8
***β* anomer**						
*β*_$^4C_1$_AB	T t t t x	−689.808466	491.0991	39.1	−690.068160	24.0
*β*_$^4C_1$_BA	T g g $\bar{g}$ x $\bar{g}$	−689.796590	489.8021	69.0	−690.057263	51.4
*β*_$^4C_1$_BC	T t t x $\bar{g}$	−689.812079	491.1969	29.7	−690.071635	15.0
*β*_$^4C_1$_CB	T g g x g $\bar{g}$	−689.803531	490.7686	51.7	−690.063384	36.2
*β*_$^4C_1$_CD	T t t x t $\bar{g}$	−689.812457	489.5455	27.1	−690.071693	13.2
*β*_$^4C_1$_DC	T g x $\bar{g}$ g $\bar{g}$	−689.805661	490.6668	46.0	−690.065579	30.4
*β*_$^4C_1$_DE	T t x t t $\bar{g}$	−689.799015	488.1239	61.0	−690.061125	39.5
*β*_$^4C_1$_ED	T$\bar{x}$ g $\bar{g}$ g $\bar{g}$	−689.815621	490.9779	20.2	−690.075345	5.1
*β*_$^4C_1$_EFA	G$\bar{x}$ t t t t	−689.814628	489.3020	21.1	−690.073657	8.4
*β*_$^4C_1$_AEF	G$\bar{t}$ g $\bar{g}$ g x	−689.816119	489.8684	17.8	−690.073585	8.6
*β*_$^1C_4$_EFA	G$\bar{x}$ $\bar{g}$ t t g	−689.820504	493.7340	10.1	−690.073050	13.8
*β*_^{O,3}B_EFC	G$\bar{x}$ $\bar{g}$ t t $\bar{g}$	−689.823429	491.2742	0.0	−690.077380	0.0
*β*_$B_{O,3}$_EFA	G$\bar{x}$ t t t t	−689.813419	489.4447	24.5	−690.072347	11.4
*β*_$B_{2,5}$_EF	G$\bar{x}$ t t $\bar{g}$ g	−689.807175	489.5532	41.0	−690.062769	36.8
*β*_$B_{1,4}$_EFA	G$\bar{x}$ g t t t	−689.811267	490.0766	30.7	−690.069134	20.5

[a] See text for details. [b] Evaluated at the B3LYP/6-31G(d,p) level. [c] Values including ZPE corrections. [d] Values obtained at the B3LYP/6-311+G(2df,2p)//B3LYP/6-31G(d,p)+ZPE level.

Table 3, we can see that for both anomers and whatever the ring conformation adopted, the relative energy differences between the various geometries are small (<52 kJ/mol) and do not vary significantly with the level of calculation. This is in favor of a mixture of several structures in the gas phase. This also suggests that the various fragmentation pathways observed upon collision may involve different initial conformations of the complex. Second, examination of Table 3 clearly indicates that the most stable $^4C_1$ structures are characterized by a formal deprotonation of the hydroxymethyl function (CH_2OH, **E**) and additional interaction with either an adjacent hydroxyl group (**D**) or a hemiacetal oxygen (**F**). It turns out that it corresponds to the deprotonation of the least acidic hydroxyl.[48] These coordination schemes are also in agreement with the specific elimination of C(1) and C(2) centers associated with the formation of the *m*/*z* 327 ion.

Globally, the cation stability appears to be governed by the nature of the deprotonated site. In the particular case of $^4C_1$ conformations, the structures are essentially bidentate and there are no evident correlations between the stability and the number of intramolecular hydrogen bonds. Moreover, concerning the **BC**, **CD**, and **DE** structures, we can see as the consequence of the exo-anomeric effect[54] that the anomeric hydroxyl remains preferentially in the g (anomer α) or $\bar{g}$ (anomer *β*) orientation (Figures 4 and 5), instead of participating in a cooperative hydrogen bonding scheme (t orientation). This effect is more pronounced as the deprotonated site gets closer to the anomeric position.

Interactions between metals and monosaccharides have been widely studied in aqueous solutions,[5] and NMR studies have revealed that metal binding to simple carbohydrates according to tridentate modes are particularly favorable, especially when

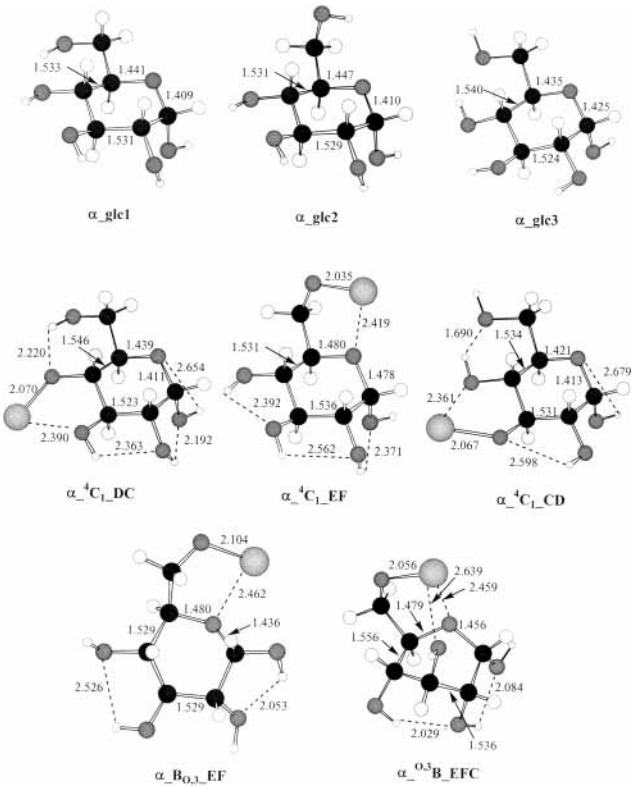

Figure 4. Cyclic forms of [Pb(α-D-glucose) − H]$^+$ complexes [bond lengths obtained at the B3LYP/6-31G(d,p) level and given in angströms].

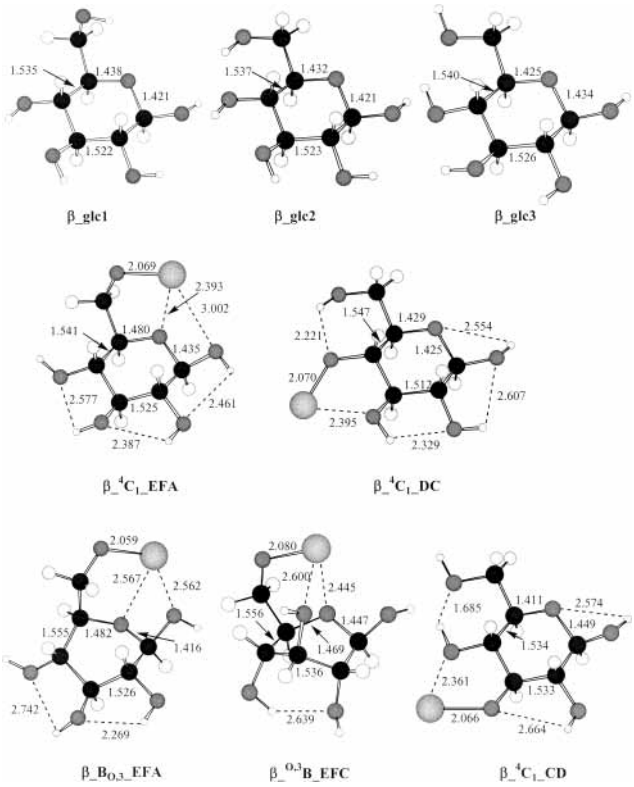

Figure 5. Cyclic forms of [Pb(β-D-glucose) − H]$^+$ complexes [bond lengths obtained at the B3LYP/6-31G(d,p) level and given in angströms].

the monosaccharide has an axial−equatorial−axial or axial−axial−axial sequence of OH groups. As this sequence is not encountered for $^4C_1$ forms, we also considered seven additional ring conformations (one chair and six boats), presented in Scheme 4, to obtain axial hydroxyl groups. The results presented in Table 3 show that, once again, the most stable geometries are those involving a deprotonated hydroxymethyl group. With these seven ring conformations, tricoordinations are more easily obtained. Furthermore, for both anomers, the most stable cyclic structure is characterized by a ^{O,3}B boat form and a tridentate interaction involving the deprotonated CH_2OH group (**E**), the hemiacetal oxygen (**F**), and the hydroxyl (**C**) borne by the carbon C(3). This particular coordination scheme (**^{O,3}B_EFC**) had also been also found to be the most favorable in the case of cationization of D-glucose by sodium ions.[51] Our calculations also emphasize the influence of intramolecular hydrogen bonds on the stability of several boat conformations. Thus, we failed in locating stable **α_^{1,4}B** and ***β*_^{1,4}B** forms. These geometries indeed collapse during the optimization step into **α_B$_{O,3}$** and ***β*_^{2,5}B** conformations, respectively, promoted by hydrogen bond strengthening. More generally, all of the boat forms obtained except ^{O,3}B geometries can be viewed as skew forms, which are intermediate between two boat conformations.

To give a picture of the distribution of charge within the [Pb(D-glucose) − H]$^+$ species, we have carried out a natural population analysis (NPA) at the B3LYP/6-31G(d,p) level by means of the NBO program for all of the structures investigated.[55] NPA charges show a transfer of electrons to the lead from the glucose moiety, the local charge on Pb ranging from 1.44 to 1.49. This value is smaller that the local charge determined for $[Pb(H_2O)_4]^{2+}$ ions (1.76−1.78),[38,56] thus indicating a greater degree of electron transfer. This analysis also reveals a slight increase of the negative charge for the interacting oxygen, accompanied by the lengthening of the corresponding C−O bonds.

Furthermore, examination of the natural bond orbitals (NBO) shows that the Pb(II) lone pair is predominantly 6s but is slightly polarized by a small 6p contribution, ranging from 3.4 to 4.7%. This feature is characterictic of hemi-directed structures, as already noticed by Bock and co-workers in their study on tetravalent lead(II) complexes,[56] but is also the signature of ionic bonds. The [Pb(D-glucose) − H]$^+$ structures would in fact correspond to [Pb^{2+} − alkoxy anion] systems. Nevertheless, natural electron configuration analysis indicates that the electron transfer is mostly in the 6p orbitals (typical values being 6s-[1.92] and 6p[0.61]$sp^{0.32}$). The value of 0.32 for Pb(II) sp hybridization is greater than the value obtained for the [Pb-$(H_2O)_4]^{2+}$ ionic complex[56] (0.16), thus suggesting a certain degree of covalency in the Pb−O bond.

Mechanisms of Elimination of $C_2H_4O_2$ and $C_4H_8O_4$ Molecules. The electron transfer from D-glucose to lead cation induces significant geometrical modifications. This is especially striking when a Pb^{2+} ion interacts with the hemiacetal oxygen (**EF** structures), as illustrated by Figures 4 and 5. To discuss this particular point, we have included in these figures the geometry of three neutral D-glucose conformers, obtained at the same level of calculations. Thus, comparison, for example, between **α_glc2** and **α_^{4}C$_1$_EF** structures demonstrates that interaction with a Pb^{2+} ion induces an important activation of the C(1)−O(5) (lengthening by 23%). This finding is in agreement with the experimental observation of cross-ring cleavages (loss of $C_nH_{2n}O_n$). Consequently, the **EF**-like complexes may correspond to the precursor ions, which, upon collision, dissociate according to cross-ring cleavages. The C(1)−O(5) bond cleavage promoted by the metallic center may therefore constitute the first step of the mechanisms of dis-

TABLE 4: Total and Relative Energies for Opened Forms of [Pb(D-glucose) − H]$^+$ Complex

structure	E_1[a] (hartree)	ZPE[a]	ΔE_1[a,b] (kJ/mol)	E_2[c] (hartree)	ΔE_2[b,c] (kJ/mol)
open1_AF	−689.800576	482.6296	153.6	−690.062953	134.7
open1_EF	−689.817930	483.2590	108.6	−690.078555	94.4
open1_ABC	−689.826941	485.2010	86.9	−690.084011	82.0
open1_BDF	−689.824720	486.2679	93.8	−690.081939	88.5
open1_ABCE	−689.820798	485.6202	103.5	−690.075548	104.7
open1_BCEA	−689.832719	486.9231	73.5	−690.086757	76.5
open1_CEBA	−689.833580	485.2887	69.6	−690.088195	71.1
open1_EABC	−689.825502	487.7040	93.2	−690.080216	94.5
open2_EA	−689.782811	483.4730	201.1	−690.045733	180.8
open2_FE	−689.788409	482.4725	185.4	−690.049018	171.2
open2_FA	−689.778287	482.3460	211.8	−690.042029	189.4
open2_FAE	−689.811013	482.9319	126.5	−690.070336	115.6
open2_FDE	−689.820696	485.4448	103.6	−690.076578	101.8
open2_FAE	−689.811105	483.6342	126.9	−690.069791	117.8
open3_EBD	−689.849790	487.1920	28.9	−690.106214	25.7
open3_EDA	−689.830077	484.9468	78.4	−690.088873	69.0
open3_EFD	−689.852561	486.1871	20.6	−690.110656	13.0
open3_ADEF	−689.856872	487.3487	10.5	−690.112877	8.4
open3_BDEF	−689.861025	487.7653	0.0	−690.116223	0.0
open3_EFBD	−689.848648	487.3666	32.1	−690.103825	32.2
β_$^{O.3}$B_EFC[d]	−689.823429	491.2742	102.2	−690.077380	105.5

[a] Evaluated at the B3LYP/6-31G(d,p) level. [b] Values including ZPE corrections. [c] Values obtained at the B3LYP/6-311+G(2df,2p)//B3LYP/6-31G(d,p)+ZPE level. [d] For the sake of comparison, the most stable cyclic structure found is also given.

SCHEME 5

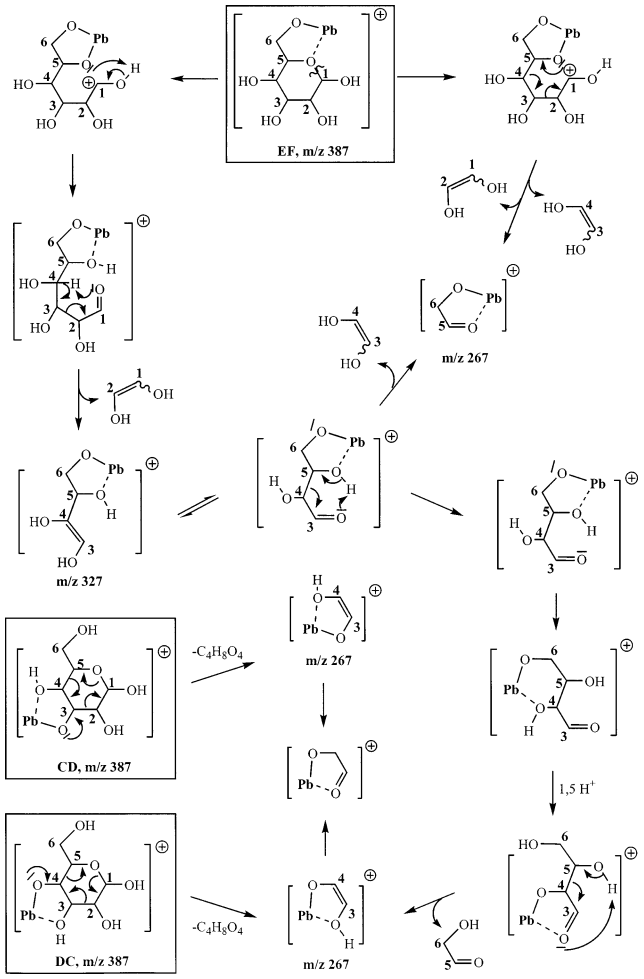

sociation proposed in Scheme 5, which also account for the details deduced from the isotope-labeling experiments.

The resulting acyclic form may undergo a proton transfer, followed by a McLafferty rearrangement, to give rise to the ion *m*/*z* 327 by loss of the C(1) and C(2) carbons. In turn, this ion expels a second $C_2H_4O_2$ [including C(3) and C(4) atoms] to generate *m*/*z* 267 ions. These latter species may also come directly from *m*/*z* 387 as evidenced experimentally.

SCHEME 6

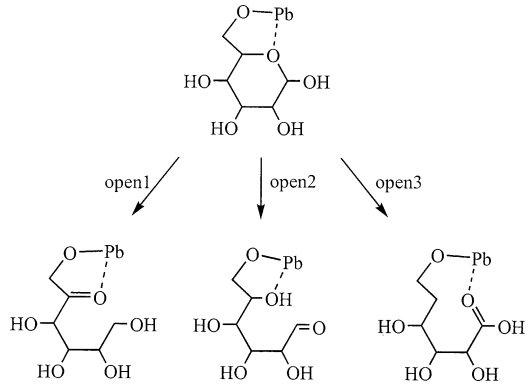

We have also demonstrated that *m*/*z* 267 ions also arise from the elimination of the C(1), C(2), C(5), and C(6) carbons. Thus, this particular fragmentation could involve a precursor *m*/*z* 387 ion in which the metallic center is bound either to C or D hydroxyl groups (Scheme 5). Indeed, we can see from Figures 4 and 5 that structures **CD** and **DC** induce lengthening of the C(2)−C(3) and C(4)−C(5) bonds, respectively, and therefore may correspond to the precursor ions. On the other hand, this fragmentation may also proceed in two steps from an **EF**-like coordinated species, via internal reorganization within the *m*/*z* 327 ion, as depicted in Scheme 5.

Opened Forms of [Pb(D-glucose) − H]$^+$ Ions. Cross-ring cleavages are the main fragmentations observed upon collision with nitrogen. Furthermore, the Pb^{2+} ion, when bound to the hydroxymethyl group and interacting with the hemiacetal oxygen, strongly activate not only the C(1)−O(5) bond but also the C(5)−O(5) bond. These two observations raise the following question: can Pb^{2+} interactions give rise to stable opened [Pb(D-glucose) − H]$^+$ structures? To address this question, we considered three modes of cleavage, as presented in Scheme 6. These three modes involve either C(1)−O(5) (**open1** and **open2**) or C(5)−O(5) (**open3**) bond cleavage, associated with 1,3H

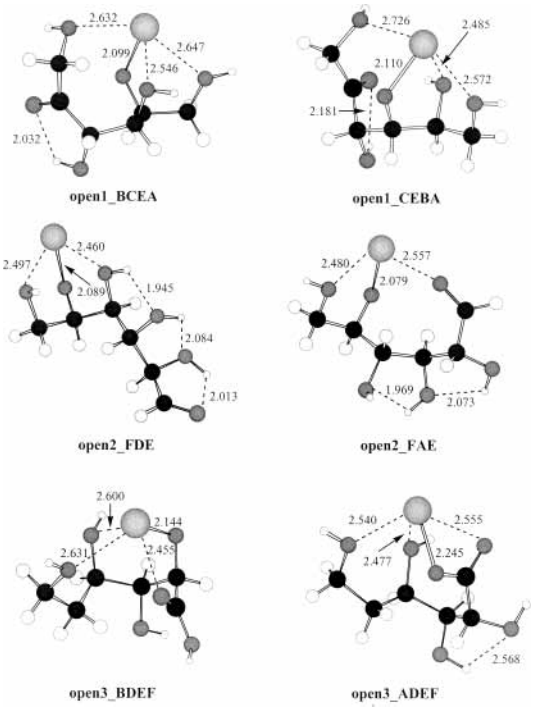

Figure 6. Relevant acyclic structures of [Pb(D-glucose) − H]$^+$ complexes (bond lengths obtained at the B3LYP/6-31G(d,p) level and given in angströms).

shifts from C(5) to C(1), from O(1) to O(5), and from C(1) to C(5), respectively.

Moreover, the second mode also corresponds to interaction between lead(II) ions and the natural open keto form of glucose. We focused on the interactions involving the terminal oxygens, which, in principle, should confer the most stability. The relative energies of the different structures considered are gathered in Table 4, and the two most stable geometries for each opening mode are given in Figure 6. Due to the greater flexibility of the carbon chain, tetradentate geometries are easily obtained. The results deduced from NBO analysis are similar to those of cyclic forms. However, unlike the cyclic complexes, Pb^{2+} interaction with the deprotonated hydroxymethyl group is not favored. The distance between the metallic center and the deprotonated hydroxyl is slightly longer (2.100−2.150 Å) than for cyclic forms (typically 2.070 Å). For the sake of comparison, Table 4 also includes the most stable cyclic geometry (***β*_^{O,3}B_EFC**). We can see that the first two modes of cleavage lead to structures that fall in the same energy range as the cyclic complexes. On the other hand, cleavage of the C(5)−O(5) generates acyclic complexes that are considerably more stable (by >100 kJ/mol for structure **open3_BDEF**) than the cyclic forms. This kind of situation has already been encountered for the Cu^+/D-glucose system.[19] Furthermore, as the most stable cyclic forms are characterized by a very strong C(5)−O(5) bond activation, one may reasonably assume that these forms, competitively with cross-ring cleavage, may collapse to **open3** complexes provided they have a sufficient amount of internal energy to cross the activation barriers associated with the 1,3H shift. Nevertheless, the other opened structures, rigorously, cannot be discarded.

Conclusion

The present study has shown that under electrospray conditions, gaseous lead(II) ions react with D-glucose to form both [Pb(D-glucose)$_m$ −H]$^+$ and [Pb(D-glucose)$_n$]$^{2+}$ complexes. MS/MS experiments on the most abundant complex, [Pb(D-glucose) − H]$^+$ (*m*/*z* 387), show that this ion essentially dissociates by cross-ring cleavages (loss of $C_2H_4O_2$ and $C_4H_8O_4$ neutrals). According to labeling experiments, the first involves specific elimination of C(1) and C(2) centers. The second corresponds to at least two distinct fragmentations and suggests that the *m*/*z* 387 ion may correspond to a mixture of several structures. This is supported by our theoretical study carried out on both pyranosic anomers. The most favorable Pb^{2+}/D-glucopyranose association, involving the metallic center attached to the deprotonated hydroxymethyl group and interacting with the hemiacetal oxygen, is characterized by strongly activated C−O ring bonds. This not only accounts for the fragmentation observed upon collision but also suggests that pyranosic complexes may also collapse to give the energetically favored acyclic structures.

Acknowledgment. We thank the Institut du Développement et des Ressources en Informatique Scientifique (IDRIS, CNRS) for computational time. We acknowledge Omicron Biochemicals for purchasing facilities. We are indebted to the Conseil General d'Ile de France for financial support. Finally, we thank Pr. O. Mó and M. Yáñez for helpful discussion.

Supporting Information Available: B3LYP/6-31G(d,p) geometry and Cartesian coordinates of the different structures investigated (bond lengths given in angströms). This material is available free of charge via the Internet at http://pubs.acs.org.

References and Notes

(1) Rhue, R. D.; Mansell, R. S.; Ou, L. T.; Cox, R.; Tang, S. R.; Ouyang, Y. *Crit. Rev. Environ. Control* **1992**, *22*, 169.
(2) Łobiński, R.; Adams, F. C. *Anal. Chim. Acta* **1992**, *262*, 285.
(3) Gorecki, T.; Pawliszyn, J. *Anal. Chem.* **1996**, *68*, 3008.
(4) Uhlenbeck, O. C.; Pan, T. *Nature* **1992**, *358*, 560.
(5) Whitfield, D. M.; Stojkovski, S.; Sarkar, B. *Coord. Chem. Rev.* **1993**, *122*, 171.
(6) Yano, S.; Otsuka, M. In *Metal Ions in Biological Systems*; Sigel, A., Sigel, H., Eds.; Dekker: New York, 1996; Vol. 32, p 28.
(7) Ekström, L. G.; Olin, Å. *Acta Chem. Scand. A* **1977**, *31*, 838.
(8) Coccioli, F.; Vicedomini, M. *J. Inorg. Nucl. Chem.* **1978**, *40*, 2103.
(9) Vesala, A.; Lönnberg, H.; Käppi, R.; Arpalahti, J. *Carbohydr. Res.* **1982**, *102*, 312.
(10) Mihalick, J. E.; Griffiths III, W. P.; Muten, J. E.; Olson, T. A.; Hein, J. B. *J. Solution Chem.* **1999**, *28*, 1019.
(11) Salpin, J.-Y.; Tortajada, J. *Adv. Mass Spectrom.* **2001**, *15*, 735.
(12) Salpin, J.-Y.; Tortajada, J.; Boutreau, L.; Haldys, V. *Eur. J. Mass Spectrom.* **2001**, *7*, 321.
(13) Salpin, J.-Y.; Tortajada, J. *J. Mass Spectrom.* **2002**, *37*, 379.
(14) Frisch, M. J.; Trucks, G. W.; Schlegel, H. B.; Scuseria, G. E.; Robb, M. A.; Cheeseman, J. R.; Zakrzewski, V. G.; Montgomery, J. A., Jr.; Stratmann, R. E.; Burant, J. C.; Dapprich, S.; Millam, J. M.; Daniels, A. D.; Kudin, K. N.; Strain, M. C.; Farkas, O.; Tomasi, J.; Barone, V.; Cossi, M.; Cammi, R.; Mennucci, B.; Pomelli, C.; Adamo, C.; Clifford, S.; Ochterski, J.; Petersson, G. A.; Ayala, P. Y.; Cui, Q.; Morokuma, K.; Malick, D. K.; Rabuck, A. D.; Raghavachari, K.; Foresman, J. B.; Cioslowski, J.; Ortiz, J. V.; Stefanov, B. B.; Liu, G.; Liashenko, A.; Piskorz, P.; Komaromi, I.; Gomperts, R.; Martin, R. L.; Fox, D. J.; Keith, T.; Al-Laham, M. A.; Peng, C. Y.; Nanayakkara, A.; Gonzalez, C.; Challacombe, M.; Gill, P. M. W.; Johnson, B. G.; Chen, W.; Wong, M. W.; Andres, J. L.; Head-Gordon, M.; Replogle, E. S.; Pople, J. A. *Gaussian 98*, revision A.7; Gaussian, Inc.: Pittsburgh, PA, 1998.
(15) Becke, A. D. *J. Chem. Phys.* **1993**, *98*, 5648.
(16) Lee, C.; Yang, W.; Parr, R. G. *Phys. Rev. B Condens. Matter* **1988**, *37*, 785.
(17) Hoyau, S.; Ohanessian, G. *Chem. Phys. Lett.* **1995**, *246*, 40.
(18) Kemper, P. R.; Weis, P.; Bowers, M. T.; Maitre, P. *J. Am. Chem. Soc.* **1998**, *120*, 13494.
(19) Alcamí, M.; Luna, A.; Mó, O.; Yáñez, M.; Boutreau, L.; Tortajada, J. *J. Phys. Chem. A* **2002**, *106*, 2641.
(20) González, L.; Mó, O.; Yáñez, M. *J. Comput. Chem.* **1997**, *18*, 1124.
(21) González, L.; Mó, O.; Yáñez, M. *J. Phys. Chem. A* **1997**, *101*, 9710.
(22) González, L.; Mó, O.; Yáñez, M. *J. Chem. Phys.* **1998**, *109*, 139.
(23) Küchle, W.; Dolg, M.; Stoll, H.; Preuss, H. *Mol. Phys.* **1991**, *6*, 1245.

(24) Salpin, J.-Y.; Tortajada, J.; Alcamí, M.; Luna, A.; Mó, O.; Yáñez, M. Manuscript in preparation.
(25) González, A. I.; Mó, O.; Yáñez, M. *J. Chem. Phys.* **2000**, *112*, 2258.
(26) Vukomanovic, D.; Stone, J. A. *Int. J. Mass Spectrom.* **2000**, *202*, 251.
(27) Jayaweera, P.; Blades, A. T.; Ikonomou, M. G.; Kebarle, P. *J. Am. Chem. Soc.* **1990**, *112*, 2452.
(28) Blades, A. T.; Jayaweera, P.; Ikonomou, M. G.; Kebarle, P. *Int. J. Mass Spectrom. Ion Processes* **1990**, *101*, 325.
(29) Blades, A. T.; Jayaweera, P.; Ikonomou, M. G.; Kebarle, P. *Int. J. Mass Spectrom. Ion Processes* **1990**, *102*, 251.
(30) Cheng, Z. L.; Siu, K. W. M.; Guevremont, R.; Berman, S. S. *J. Am. Soc. Mass Spectrom.* **1992**, *3*, 281.
(31) Peschke, M.; Blades, A. T.; Kebarle, P. *J. Phys. Chem. A* **1998**, *102*, 9978.
(32) Rodriguez, S. E.; Jockusch, R. A.; Williams, E. R. *J. Am. Chem. Soc.* **1999**, *121*, 8898.
(33) Peschke, M.; Blades, A. T.; Kebarle, P. *J. Am. Chem. Soc.* **2000**, *122*, 10440.
(34) Beyer, M.; Williams, E. R.; Bondybey, V. E. *J. Am. Chem. Soc.* **1999**, *121*, 1565.
(35) Cotton, F. A.; Wilkinson, G.; Murillo, C. A.; Bochmann, M. *Advanced Inorganic Chemistry*, 6th ed.; Wiley-Interscience: New York, 1999.
(36) Shvarstburg, A.; Siu, K. W. M. *J. Am. Chem. Soc.* **2001**, *123*, 10071.
(37) Nimal Perera, W.; Hefter, G.; Sipos, P. M. *Inorg. Chem.* **2001**, *40*, 3974 and ref 37 cited therein.
(38) Akibo-Betts, G.; Barran, P. E.; Puskar, L.; Duncombe, B.; Cox, H.; Stace, A. J. *J. Am. Chem. Soc.* **2002**, *124*, 9257.
(39) Pearson, R. G. *Chem. Ber.* **1967**, *3*, 103.
(40) Fura, A.; Leary, J. A. *Anal. Chem.* **1993**, *65*, 2805.
(41) Carlesso, V.; Afonso, C.; Fournier, F.; Tabet, J. C. *Int. J. Mass Spectrom.* **2002**, *219*, 559.
(42) Smith, G.; Leary, J. A. *J. Am. Chem. Soc.* **1998**, *120*, 13046.
(43) Smith, G.; Kaffashan, A.; Leary, J. A. *Int. J. Mass Spectrom.* **1999**, *182/183*, 299.
(44) Gaucher, S. P.; Leary, J. A. *Anal. Chem.* **1998**, *70*, 3009.
(45) Gaucher, S. P.; Leary, J. A. *Int. J. Mass Spectrom.* **2000**, *197*, 139.
(46) Carlesso, V.; Fournier, F.; Tabet, J. C. *Eur. J. Mass Spectrom.* **2000**, *6*, 421.
(47) Domon, B.; Costello, C. E. *Glycoconjugate J.* **1988**, *5*, 397.
(48) Mulroney, B.; Peel, J. B.; Traeger, J. C. *J. Mass Spectrom.* **1999**, *34*, 544.
(49) Cole, R. B. *J. Mass Spectrom.* **2000**, *35*, 763.
(50) Collins, P.; Ferrier, R. *Monosaccharides: Their Chemistry and Their Role in Natural Products*; Wiley: Chichester, U.K., 1995.
(51) Cerda, B. A.; Wesdemiotis, C. *Int. J. Mass Spectrom.* **1999**, *189*, 189.
(52) (a) Stewart, J. J. P. *J. Comput. Chem.* **1989**, *10*, 209. (b) Hyperchem release 6.01 for Windows; Hypercube, Inc., 1999.
(53) Cramer, C. J.; Truhlar, D. G. *J. Am. Chem. Soc.* **1993**, *115*, 5745.
(54) Lemieux, R. U.; Pavia, A. A.; Martin, J. C.; Watanabe, K. A. *Can. J. Chem.* **1969**, *47*, 4427.
(55) Glendening, E. D.; Reed, A. E.; Weinhold, F. NBO version 3.1.
(56) Shimony-Livny, L.; Glusker, J. P.; Bock, C. W. *Inorg. Chem.* **1998**, *37*, 853.